

Use of the near infrared similarity reflectance spectrum for the quality control of remote sensing data

Kevin Ruddick^{*a}, Vera De Cauwer^{ab} and Barbara Van Mol^a

^aManagement Unit of the North Sea Mathematical Models (MUMM), Royal Belgian Institute for Natural Sciences (RBINS), 100 Gulledele, B-1200 Brussels, Belgium;

^bNow at Greenmap, PB 2404 Swakopmund, Namibia

ABSTRACT

The shape of water-leaving reflectance spectra in the near infrared range 700-900nm is almost invariant for turbid waters and has been analysed and tabulated as a similarity spectrum by normalisation at 780nm. This similarity spectrum is used here for the quality control of seaborne reflectance measurements and for the improvement of sky glint correction. Estimates of the reflectance measurement error associated with imperfect sky glint correction from two different wavelength pairs are shown to be nearly identical. A demonstration of residual reflectance correction for data collected in cloudy, high wave conditions has shown that this correction removes a large source of variability associated with temporal variation of the wave field. The error estimate applied here to seaborne measurements has wide-ranging generality and is appropriate for any water-leaving reflectance spectra derived from seaborne, airborne or satellite borne sensors provided suitable near infrared bands are available.

Keywords: near infrared, water-leaving reflectance, turbid water, sky glint, quality control, remote sensing, atmospheric correction

1. INTRODUCTION

1.1 Near infrared aquatic optical properties and the similarity spectrum

In the near infrared (NIR) range of the electromagnetic spectrum pure water absorption is much larger than other sources of aquatic absorption such as phytoplankton, non-algae particles and coloured dissolved organic matter (CDOM). This simplifies greatly the analysis of aquatic optical properties and yields the important result that the spectral reflectance of turbid water bodies can be well represented by a single free parameter, such as the magnitude of reflectance for a single wavelength¹ or the total scattering coefficient². The spectral shape can be represented by a general "similarity" spectrum, which is defined as the spectral reflectance normalised at a reference wavelength and which is valid over a wide range of conditions¹. A corollary of this result is that reflectance ratios are almost invariant in the near infrared, except if reflectance is very high, a fact that has been exploited in various forms for the atmospheric correction of ocean colour data over turbid waters³⁻⁷.

This similarity spectrum has been tabulated and analysed initially for turbid coastal waters using seaborne reflectance measurements¹. However, its range of validity should be much larger. In principle the same spectrum should be valid also for most inland waters, since water absorption is thought to be almost invariant with respect to salinity variations⁸. Exceptions to validity include situations where floating layers are present or where bottom reflection is significant at near infrared wavelengths (extremely shallow water).

Characterisation of the near infrared water-leaving reflectance via the similarity spectrum provides crucial input data for algorithms to correct spaceborne and airborne remote sensing data over turbid waters and can also be used for the quality

* K.Ruddick@mumm.ac.be; phone +32 2 7732131; fax +32 2 7706972; www.mumm.ac.be/OceanColour

control of water-leaving reflectance spectra derived from spaceborne, airborne and seaborne remote sensing. The former application has been outlined previously¹. The latter application is the focus of the present paper.

In this paper the near infrared similarity spectrum is used to estimate the measurement error owing to imperfect correction of sky reflection at the air-water interface in the processing of water-leaving reflectance measurements. While the method described is demonstrated using measurements made above water from a ship, exactly the same method can be applied to assess the quality of *any* water-leaving reflectance measurements, including atmospherically-corrected spaceborne and airborne measurements. The potential range of application is thus very significant.

1.2 Theoretical background

The water-leaving reflectance, ρ_w , is defined for wavelength λ by:

$$\rho_w(\lambda) = \frac{\pi L_w^{0+}(\lambda)}{E_d^{0+}(\lambda)} \quad (1)$$

where L_w^{0+} is the water-leaving radiance just above the air-water interface after correction for radiance reflected at the air-water interface and E_d^{0+} is the downwelling irradiance just above the air-water interface. Taking a reference wavelength of 780nm, chosen because of the low temperature-related variability^{9,10} of pure water absorption at this wavelength, ρ_w can be approximated in the near infrared by:

$$\rho_w(\lambda) = \rho_w(780\text{nm}) \rho_{wn780}(\lambda) \quad (2)$$

where the similarity spectrum $\rho_{wn780}(\lambda)$ is considered as constant for most water bodies and has been tabulated based on seaborne reflectance measurements¹.

The approximation (2) has been shown¹ by theory, radiative transfer simulation and seaborne measurements to be valid to within a few per cent for the spectral range 700-900nm for a wide range of turbid water bodies with reflectances from about 0.0001 to 0.03. At lower reflectances, for very clear water, the similarity spectrum must be modified to account for the backscatter of pure water which varies with wavelength differently from particulate backscatter. At higher reflectances, for extremely turbid water, reflectance is no longer linearly related to backscatter even in the near infrared^{5,11} and the approximation (2) can only be used for the spectral range where reflectance does not exceed about 0.03. Possible variability of the tabulated similarity spectrum caused by temperature variation of pure water absorption, spectral variation of particulate backscatter, particulate or coloured dissolved organic matter absorption and viewing geometry has been investigated and demonstrated¹ to be limited to a few per cent for most situations relevant to remote sensing.

2. METHOD

2.1 Test region

Uses of the NIR similarity spectrum for turbid waters are demonstrated here using above water reflectance measurements collected from the oceanographic research vessels Belgica (51m) and Zeeleeuw (56m) during 22 cruises (64 days, 246 stations) in the period 2001-2004 (March-September each year). Measurements were made in Belgian waters and in the waters of neighbouring states (UK, France, Netherlands) in the Southern Bight of the North Sea and the Eastern Channel. For these measurements total water depth ranged from about 9m (limited by the draught of the ships) up to 57m with most measurements made in fairly shallow turbid water (e.g. median water depth of about 20m, Secchi depth of about 3m). Optical conditions in these waters are described in various references relating to optical remote sensing of suspended particulate matter^{12,13} and chlorophyll *a* concentration¹⁴⁻¹⁶, turbid water atmospheric correction⁶ and validation of ocean colour sensors^{17,18}.

2.2 Measurement technique and instrumentation

Water-leaving reflectance is calculated from simultaneous above water measurements of E_d^{0+} , total upwelling radiance (i.e. from the water and from the air-sea interface) at a zenith angle of 40° , L_{sea}^{0+} , and sky radiance, L_{sky}^{0+} , in the direction of the region of sky which reflects into the sea-viewing sensor, by:

$$\rho_w = \pi \frac{L_{sea}^{0+} - \rho_{sky} L_{sky}^{0+}}{E_d^{0+}} \quad (3)$$

where ρ_{sky} is the air-water interface reflection coefficient for radiance, equal to the Fresnel reflection coefficient in the case of a flat sea surface. This corresponds to “Method 1” of the NASA protocols¹⁹. Measurements are performed with three TriOS-RAMSES hyperspectral spectroradiometers, two measuring radiance and one measuring downwelling irradiance. The instruments are mounted on a steel frame²⁰ as shown in Figure 1; zenith angles of the sea- and sky-viewing radiance sensors are 40° . The frame is fixed to the prow of the ship, facing forwards to minimise ship shadow and reflection²¹. The ship is manoeuvred on station to point the radiance sensors at a relative azimuth angle of 135° away from the sun. Lenses are checked and if necessary cleaned prior to each measurement. Measurements are made for 10 minutes, taking a scan of the three instruments every 10 s. The sensors measure over the wavelength range 350-950nm with sampling interval of approximately 3.3 nm and spectral width of about 10 nm. Position is measured simultaneously by GPS. Data is acquired with the MSDA software using the file recorder function and is radiometrically calibrated using nominal calibration constants. Calibrated data for E_d^{0+} , L_{sea}^{0+} and L_{sky}^{0+} are interpolated to 2.5nm intervals and exported to Excel for further processing. The sensors are calibrated in a MERIS Validation Team laboratory every year after which the definitive spectra are obtained. The measurement sequence of scanning every 10s for 10 minutes produces a time series of 60 scans. Scans are flagged for rejection if any of the following cases occurs:

- Inclination from the vertical exceeds 5%
- E_d^{0+} , L_{sky}^{0+} or L_{sea}^{0+} at 550nm differs by more than 25% from either neighbouring scan
- Incomplete or discontinuous spectra (occasional instrument malfunction)

Finally, the water-leaving reflectances measured from the first five scans passing these tests are mean averaged to yield the water-leaving reflectance and its standard deviation for each station.



Figure 1 System of three spectroradiometers installed on a steel frame at the prow of the Research Vessel Zeeleeuw.

2.3 Correction of air-water interface reflection

It is well-established²² that a major source of uncertainty in above water seaborne measurements of water-leaving reflectance is the correction for light reflected at the air-water interface, commonly called skylight reflection or sky glint. In the method described in section 2.2, which is based on Method 1 of the NASA/SeaWiFS protocols¹⁹, this sky glint correction has been estimated based on radiative transfer simulations²³. These simulations have been approximated to represent ρ_{sky} as a function of wind speed at 10m above the air-water interface for clear, sunny sky conditions. For uniform overcast conditions a constant value of ρ_{sky} is adopted. The choice of which ρ_{sky} parameterisation to use has been defined here according to the magnitude of $L_{sky}(750nm)/E_d^{0+}(750nm)$ which takes a value of about 0.02 in the clear sky simulations²³, but reaches much higher values, e.g. of order 0.3, for fully overcast conditions. Thus,

$$\rho_{sky} = 0.0256 + 0.00039 * W + 0.000034 * W^2 \quad \text{for} \quad \frac{L_{sky}(750nm)}{E_d^{0+}(750nm)} < 0.05 \quad (4)$$

$$\rho_{sky} = 0.0256 \quad \text{for} \quad \frac{L_{sky}(750nm)}{E_d^{0+}(750nm)} \geq 0.05 \quad (5)$$

These parameterisations are designed for the ideal cases of clear, sunny sky or alternatively fully overcast sky. The intermediate case of partly cloudy skies is particularly troublesome, especially if scattered clouds are present in or near the portion of sky viewed by the sky-viewing sensor²³. In such a case neither (4) nor (5) can be expected to perform well *a priori* and the whole measurement concept is flawed, because sky glint cannot be accurately estimated from the measurement of L_{sky} made in a single direction.

2.4 Estimation of error in correction of air-water interface reflection

Above water reflectance measurement procedures such as that described in section 2.2 and 2.3 using an estimation of ρ_{sky} based on wind speed and/or viewing geometry, have been used previously with minor variations by many investigators²⁴⁻²⁸. An alternative approach to such independent modelling of ρ_{sky} is the use of the sky and water radiance measurements to estimate the air-water interface correction by supposing that water-leaving reflectance is zero at a reference near infrared wavelength²⁹. Many variants on these approaches exist, including hybrid approaches²⁴ where ρ_{sky} is estimated as the smooth surface Fresnel reflection correction but a further wavelength-independent ‘‘residual’’ correction is made based on the assumption of zero water-leaving reflectance at a near infrared wavelength, e.g. 780nm. A further class of methods reduces sky glint by viewing at the Brewster angle through a vertical polarizer^{30, 31} and correcting any residual sky glint by supposing that water-leaving reflectance at 870nm is zero. A selection of sky glint correction methods have been intercompared²² and more information on the possible variants can be found in the references found therein and in the NASA/SeaWiFS protocols document¹⁹.

It is noted²² also that a sky glint correction method depends not only on the formula used for evaluation of ρ_{sky} , but also on details of the filtering and averaging of measurements. In this respect instruments which sample very rapidly the water surface (i.e. faster than wave-induced temporal variations of upwelling radiance) and for a narrow field of view can use temporal filters which remove more efficiently both sun glint and sky glint from waves giving high reflection, thus reducing the magnitude and surface wave dependence of the air-water interface reflection and hence measurement uncertainties. However, hyperspectral instruments based on CCD spectrometers, such as those used here, generally require longer integration time, e.g. 1-2s, and thus measurements represent a temporal average over differently oriented wave facets which cannot be entirely filtered out.

It is well-recognised that methods based on the assumption of zero water-leaving reflectance at a near infrared wavelength are seriously flawed for turbid waters where this assumption no longer holds. The present paper proposes a more generally valid assumption based on the NIR similarity spectrum can be used either to assess the quality of

measurements based on parameterisation of ρ_{sky} or to improve the accuracy of measurements based on residual corrections using NIR wavelengths. The approach is analogous in many ways to algorithms developed for the atmospheric correction of satellite data for turbid waters and is similar to an algorithm proposed³² for air-water interface correction using measurements at 715nm and 735nm.

In a first step it is assumed that the measurement error in the NIR can be represented by an error, ε , which is spectrally flat as is typical of air-water interface correction errors over limited wavelength ranges³² and as supposed in methods employing a “residual” correction. Thus, the true water-leaving reflectance, ρ_w is related to the measured water-leaving reflectance, ρ_w^m by:

$$\rho_w(\lambda) = \rho_w^m(\lambda) - \varepsilon \quad (6)$$

It is also assumed that $\rho_w(\lambda)$ can be approximated by the similarity spectrum (2) at least for two suitably chosen NIR wavelengths, λ_1 and λ_2 . Thus,

$$\frac{\rho_w(\lambda_1)}{\rho_w(\lambda_2)} = \frac{\rho_{wm780}(\lambda_1)}{\rho_{wm780}(\lambda_2)} = \alpha_{1,2} \quad (7)$$

where $\alpha_{1,2}$ can be read from the tabulated similarity spectrum¹. Then by combining (6) and (7), ε can be estimated as:

$$\varepsilon = \frac{\alpha_{1,2}\rho_w^m(\lambda_2) - \rho_w^m(\lambda_1)}{\alpha_{1,2} - 1} \quad (8)$$

This is illustrated in Figure 2.

2.5 Choice of wavelength for error estimation

The choice of wavelength to be used for estimation of ε is made intuitively according to a number of considerations:

- $\alpha_{1,2}$ should be significantly different from one so that the water reflectance has a different colour from the supposed white measurement error enabling the two components to be separated (the denominator of (8) should be significantly non-zero).
- The range 755-770nm is avoided because of possible problems associated with atmospheric oxygen absorption.
- The range 734-758nm is avoided because of variation of pure water absorption, and hence the similarity spectrum, with temperature³³.
- Wavelengths lower than 720nm are avoided because of relatively higher standard deviation noted for the measurements used to calculate the similarity spectrum, possibly caused by variations in absorption from non-algae particles and/or CDOM.
- Wavelengths higher than 890nm are avoided because atmospheric water vapour absorption renders satellite remote sensing less useful near 900nm and because the similarity spectrum has not yet been measured above 900nm.

Subject to these constraints the two wavelength pairs $(\lambda_1, \lambda_2) = (720\text{nm}, 780\text{nm})$ and $(780\text{nm}, 870\text{nm})$ have been chosen to cover distinct parts of the NIR spectrum and thus yield as far as possible independent estimates of ε . These two estimates are denoted as $\varepsilon(720\text{nm}, 780\text{nm})$ and $\varepsilon(780\text{nm}, 870\text{nm})$ respectively and are calculated using $\alpha_{1,2} = 2.35$ and 1.91 respectively.

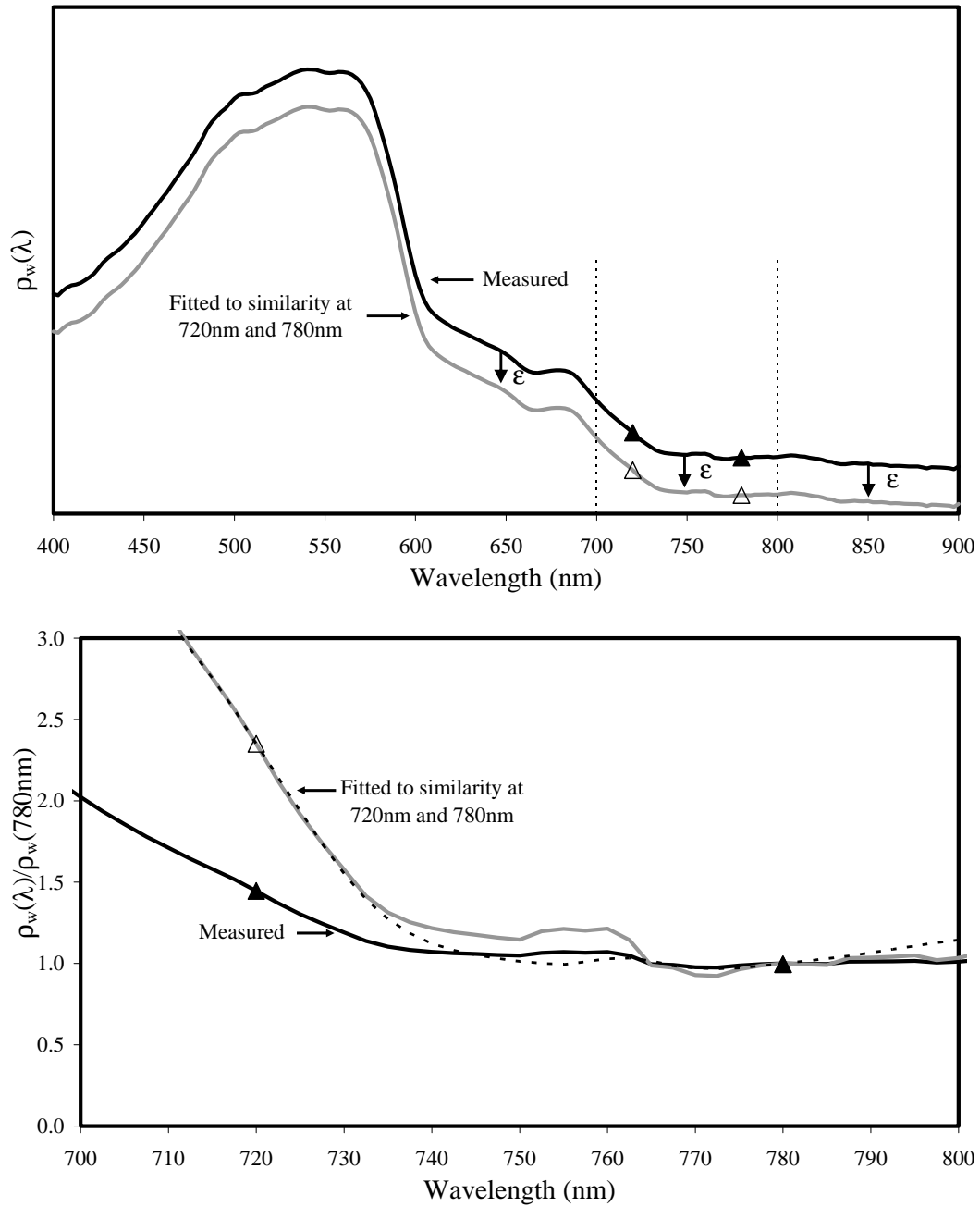


Figure 2 Schematic showing the white correction needed to make measured spectrum conform to the similarity spectrum for the wavelength pair (720nm,780nm). The solid black line represents a measured spectrum with solid triangles marking the measured reflectance at 720nm and 780nm. The solid grey line represents the measured spectrum after white correction ϵ needed to fit the similarity spectrum at 720nm and 780nm and the hollow triangles represent the corresponding data values at 720nm and 780nm. (top) Water-leaving reflectance, ρ_w ; (bottom) Water-leaving reflectance normalised at 780nm, $\rho_{w|780}$. Note the change in x axis in the two figures as marked by the dashed vertical lines in the top panel. In the bottom panel the full similarity spectrum is given as a dashed line.

3. RESULTS

3.1 Comparison of error estimate for different wavelength pairs

For each of the 246 stations where measurements have been recorded the white measurement error ε has been estimated as described in sections 2.4 and 0. The two estimates $\varepsilon(720nm, 780nm)$ and $\varepsilon(780nm, 870nm)$ are plotted together in Figure 3. There is a very strong correlation between these two estimates with regression slope almost equal to one. This gives some confidence in the reliability of the proposed error estimate and in the assumption of a white measurement error at least for the spectral range 720-870nm considered. The most important outliers in Figure 3 are all stations where $\rho_w(720nm) > 0.03$. In such conditions the measured $\rho_w(720nm)/\rho_w(780nm)$ is expected to be less than its tabulated value because of the high reflectance “saturation” effect⁵ and $\varepsilon(720nm, 780nm)$ will be overestimated.

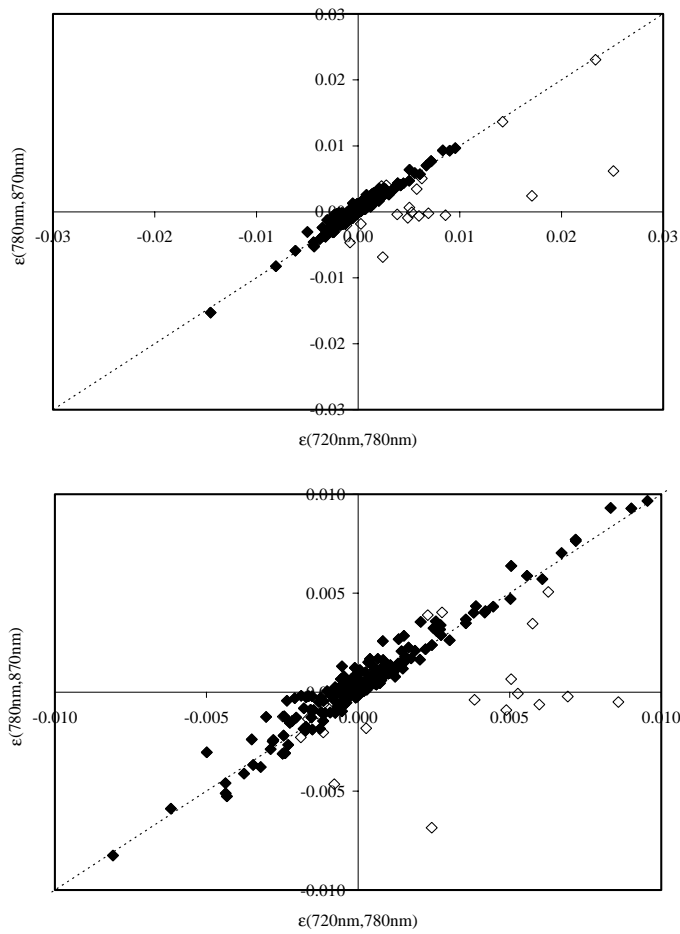


Figure 3. Scatterplot of the two estimates of reflectance measurement error, $\varepsilon(720nm, 780nm)$ and $\varepsilon(780nm, 870nm)$: (top) for all stations, (bottom) with x and y axes limited to the range (-0.01,0.01). Solid diamonds have $\rho_w(720nm) < 0.03$, within the range of applicability of the similarity spectrum. Hollow diamonds have $\rho_w(720nm) \geq 0.03$ and $\varepsilon(720nm, 780nm)$ is thus less reliable for these points. The 1-1 line passing through the origin is shown as a dotted line.

3.2 Quality control of seaborne reflectance measurements

In the context of quality control of seaborne reflectance measurements an estimate of $\varepsilon(720nm,780nm)$ or $\varepsilon(780nm,870nm)$ could be compared with the absolute value of measured water-leaving reflectance, possibly at shorter non-NIR wavelengths such as 555nm or 670nm, to obtain an estimate of the relative measurement error associated with sky glint correction. In cases where this error exceeds a target threshold the measurement would be discarded as unusable for the specified application. As an example, a target of total measurement uncertainty not exceeding 5% has been set for the seaborne validation of water-leaving reflectance from SeaWiFS³⁴. Less ambitious targets could be acceptable for other applications, such as the detection of high biomass algae blooms from airborne or satellite data, but the same principle of estimating the sky glint correction error from (8) remains entirely appropriate.

Figure 4 shows a comparison between the estimated white error $\varepsilon(720nm,780nm)$ and $\rho_w(670nm)$ for stations where $\rho_w(720nm) < 0.03$. The points are sorted according to optimal and suboptimal measurement conditions. For reference a 5% relative error line is shown, though it is noted that the air-water interface correction is only one source of total measurement uncertainty and points lying within the 5% region cannot thus be considered as satisfying the condition of <5% total measurement uncertainty. This figure shows that nearly all points with high relative error as estimated from $\varepsilon(720nm,780nm)$ correspond in some way to suboptimal measurements either because wind speed exceed 10 m/s, or because the sky is not clear and sunny or because standard deviation of $\rho_w(670nm)$ for the 5 scans exceeded 10% of the average over the 5 scans. This suggests some degree of correspondence between the new quality control criterion based on $\varepsilon(720nm,780nm)$ and existing notions of good measurement conditions.

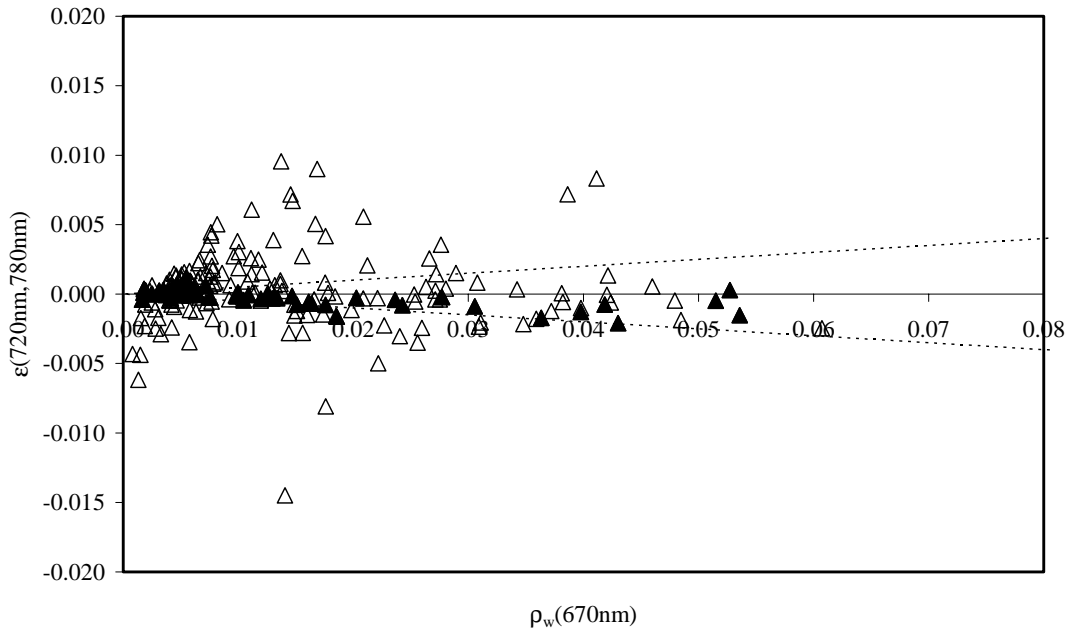


Figure 4. Comparison of the estimated air-sea interface correction error $\varepsilon(720nm,780nm)$ with absolute reflectance, $\rho_w(670nm)$. Only stations with $\rho_w(720nm) < 0.03$ are shown here because $\varepsilon(720nm,780nm)$ may be unreliable for higher reflectances. Solid triangles represent stations with optimal conditions: wind speed less than 10 m/s, sunny sky as denoted by $L_{sky}(750nm)/E_d^{0+}(750nm) < 0.05$ and standard deviation of $\rho_w(670nm)$ for the 5 scans less than 10% of the average over the 5 scans. Hollow triangles represent all other stations. The region of 5% relative error is shown as a dotted line.

3.3 Improvement of water-leaving reflectance measurements in overcast conditions

In the previous section the use of (8) was proposed only as part of the quality control of measurements and the similarity spectrum was not used in the estimation of ρ_w . An alternative use of the similarity spectrum is to *improve* the estimation of ρ_w thus extending to turbid waters methods such as those cited in section 2.4 which used the clear water assumption of zero NIR water-leaving reflectance for residual correction of ρ_w measurements. Thus, from a first estimate of ρ_w^m the error estimate ε is calculated and (6) is used to correct, and hopefully improve, the first estimate of ρ_w^m . If such an approach is followed it is no longer possible to use the same ε estimate for independent quality control as was used for estimation of ρ_w and an important element of quality control is lost. Such an approach is, therefore, probably not appropriate for the high quality reflectance measurements needed for ocean colour satellite validation but may be useful for improving data for, say, algae bloom detection, particularly in overcast conditions.

A preliminary illustration of such an approach is shown in Figure 5, where the 5 scans used to calculate average reflectance are shown both from the standard method and after subsequent application of a correction using (6) where ε is calculated individually for each scan from wavelengths 720nm and 780nm. For this station wind speed was recorded as 10.3 m/s, wave height was estimated visually as 1.5m, cloud cover as 7/8, mainly grey cumulus, and the sun was clouded. The component of radiance recorded by the sea-viewing sensor arising from air-water interface reflection was estimated as 34%, 63% and 87% at 555nm, 670nm and 780nm respectively.

In this case the correction provided by using $\varepsilon(720nm, 780nm)$ has proved effective in greatly reducing the variability over the 5 scans, especially for the red and near infrared wavelengths where one scan yielded previously clearly erroneous negative reflectance data. In general the water-leaving reflectance should be rather invariant over the 5 scans unless a marine front passes through the measurement volume. It is, thus, thought that the variability over the 5 scans in this case is caused primarily by variation in sky glint reflection because of variation in the orientation of wave facets. The use of $\varepsilon(720nm, 780nm)$ allows most of this wave-induced variability to be removed yielding a more constant estimation of the water-leaving reflectance. Some variability remains for blue and green wavelengths indicating that further work is required to improve measurements there, possibly by considering the wavelength variation of air-sea interface reflection and possibly using the measurements of L_{sky}/E_d^{0+} to estimate a non-white ε .

The variability between scans shown in Figure 5 is typical of measurements made in high wind, cloudy conditions. In the case of measurements made in optimal sunny conditions the variability between scans is much smaller and it is probably preferable to avoid this extra white correction to data, retaining the use of the similarity spectrum for independent quality control as described in section 3.2.

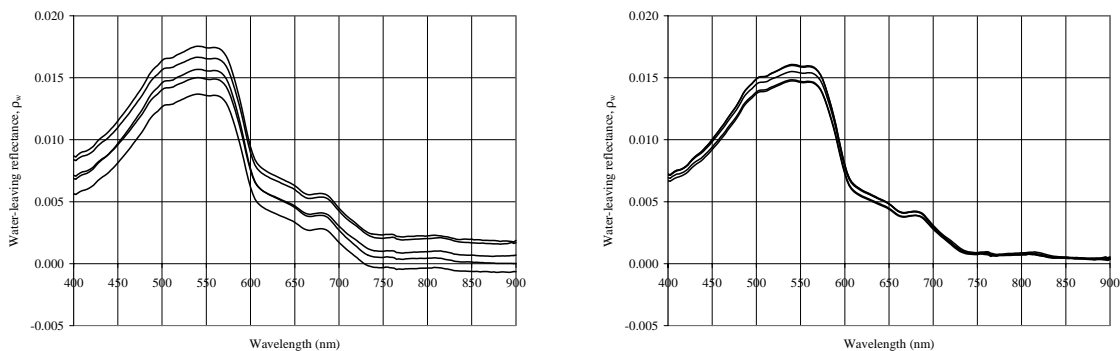


Figure 5 The five scans used for water-leaving reflectance measurement at a station typical of cloudy sky with high waves. Measurements were made at 12:39 UTC on 5th September 2001 at (51° 27.53' N, 2° 37.94' E). (left) The first estimates of ρ_w and (right) corrected estimates using (6) with $\varepsilon(720nm, 780nm)$.

4. CONCLUSIONS

This paper has described the use of the similarity spectrum for NIR water-leaving reflectance in turbid waters for the quality control of seaborne reflectance measurements (e.g. for validation of ocean colour satellites) and for the improvement of sky glint correction of such measurements (e.g. for improvement of airborne or seaborne measurements in overcast conditions). Estimates of the reflectance measurement error associated with imperfect sky glint correction from two different wavelength pairs are shown to be nearly identical giving confidence in the method. Comparison of the error estimate with conditions known to be favourable/unfavourable for above water reflectance measurements shows that this estimate corresponds with existing notions of good conditions. Finally a demonstration of residual reflectance correction for data collected in cloudy, high wave conditions has shown that this correction removes a very large source of variability associated with temporal variation of the wave field.

While applied here in the context of seaborne reflectance measurements the same error estimate, as represented by (8) and the tabulated similarity spectrum¹, can be used much more generally for the quality control of remote sensing data originating from aircraft or satellites. In fact, thanks to the general nature of the NIR similarity spectrum almost all water-leaving reflectance spectra acquired for water bodies have the same shape within the NIR range 700-900nm to within a few per cent. This fact is already used for selected wavelength pairs for the atmospheric correction of ocean colour data for turbid waters, e.g. for 765nm and 865nm for SeaWiFS, and cannot therefore be reused for the same wavelength pair for quality control. However, if sufficient (3 or more) and suitable chosen NIR wavelengths are available, it is still possible to retain one NIR wavelength pair for independent quality control of the atmospheric correction.

ACKNOWLEDGEMENTS

This study was funded by the Belgian Science Policy Office's STEREO programme in the framework of the BELCOLOUR project SR/00/03. The captains, crew and support staff of the Research Vessels Belgica and Zeeleeuw are thanked for their enthusiastic help with the seaborne measurements. Gerald Moore and Youngje Park are acknowledged for discussions regarding the NIR similarity spectrum.

REFERENCES

1. Ruddick, K. G., De Cauwer, V., Park, Y. & Moore, G. "Seaborne measurements of near infrared water-leaving reflectance - the similarity spectrum for turbid waters", *Limnology and Oceanography* (submitted), 2005.
2. Sydor, M., Wolz, B. D. & Thralow, A. M. "Spectral analysis of bulk reflectance from coastal waters: Deconvolution of diffuse spectra due to scattering and absorption by coastal water", *Journal of Coastal Research*, **18**, 352-361, 2002.
3. Arnone, R. A., Martinolich, P., Gould, R. W., Stumpf, R. & Ladner, S. "Coastal optical properties using SeaWiFS". *Ocean Optics XIV (CDROM)*, Office of Naval Research, Washington, D.C., 1998.
4. Hu, C., Carder, K. L. & Muller-Karger, F. "Atmospheric correction of SeaWiFS imagery over turbid coastal waters: a practical method", *Remote Sensing of the Environment*, **74**, 195-206, 2000.
5. Moore, G. F., Aiken, J. & Lavender, S. J. "The atmospheric correction of water colour and the quantitative retrieval of suspended particulate matter in Case II waters: application to MERIS", *International Journal of Remote Sensing*, **20**, 1713-1734, 1999.
6. Ruddick, K. G., Ovidio, F. & Rijkeboer, M. "Atmospheric correction of SeaWiFS imagery for turbid coastal and inland waters", *Applied Optics*, **39**, 897-912, 2000.
7. Siegel, D. A., Wang, M., Maritorena, S. & Robinson, W. "Atmospheric correction of satellite ocean color imagery: the black pixel assumption", *Applied Optics*, **39**, 3582-3591, 2000.
8. Pegau, W. S., Gray, G. & Zaneveld, J. R. "Absorption and attenuation of visible and near-infrared light in water: dependence on temperature and salinity", *Applied Optics*, **36**, 6035-6046, 1997.
9. Buiteveld, H., Hakvoort, J. M. H. & Donze, M. "The optical properties of pure water". *Ocean Optics XII*, ed. Jaffe, J. S., 174-183, SPIE, 1994.
10. Hollis, V. S. *Non-invasive monitoring of brain tissue temperature by near-infrared spectroscopy*, PhD Thesis, University College London, pp240, 2002.

11. Lavender, S. J., Pinkerton, M. H., Moore, G. F., Aiken, J. & Blondeau-Patissier, D. "Modification to the atmospheric correction of SeaWiFS ocean colour images over turbid waters", *Continental Shelf Research*, **25**, 539-555, 2005.
12. Nechad, B., De Cauwer, V., Park, Y. & Ruddick, K. "Suspended Particulate Matter (SPM) mapping from MERIS imagery. Calibration of a regional algorithm for the Belgian coastal waters", *MERIS user workshop held in Frascati, Special Publication SP-549*, European Space Agency, Frascati, 2003.
13. Nechad, B., Van Den Eynde, D., Fettweis, M. & Francken, F. "Suspended particulate matter mapping from multitemporal SeaWiFS imagery over the Southern North Sea - SEBAB project", *Second International Workshop on the Analysis of multi-temporal remote sensing images (Multitemp 2003)*, eds. Smits, P. C. & Bruzzone, L., 357-367, World Scientific Publishing, Ispra, 2004.
14. De Cauwer, V., Ruddick, K., Park, Y., Nechad, B. & Kyramarios, M. "Optical remote sensing in support of eutrophication monitoring in the Southern North Sea", *EARSeL eProceedings*, **3**, 208-221, 2004.
15. Gons, H. J., Rijkeboer, M., Bagheri, S. & Ruddick, K. G. "Optical teledetection of chlorophyll-*a* in estuarine and coastal waters", *Environmental Science and Technology*, **34**, 5189-5192, 2000.
16. Ruddick, K., Park, Y. & Nechad, B. "MERIS imagery of Belgian coastal waters: mapping of Suspended Particulate Matter and Chlorophyll-*a*" *MERIS user workshop held in Frascati, Special Publication SP-549*, European Space Agency, Frascati, 2003.
17. Park, Y., De Cauwer, V., Nechad, B. & Ruddick, K. "Validation of MERIS water products for Belgian coastal waters: 2002-2003", *MERIS and AATSR Calibration and Geophysical Validation workshop held in Frascati, Special Publication WPP-223*, European Space Agency, Frascati, 2003.
18. Ruddick, K. et al. "Preliminary validation of MERIS water products for Belgian coastal waters", *Envisat Validation workshop held in Frascati, Special Publication SP-531*, European Space Agency, Frascati, 2002.
19. Mueller, J. L. et al. "Above-water radiance and remote sensing reflectance measurements and analysis protocols". *Ocean Optics protocols for satellite ocean color sensor validation Revision 2*, 98-107, National Aeronautical and Space Administration, Greenbelt, Maryland, 2000.
20. Hooker, S. B. & Lazin, G. "The SeaBOARR-99 Field Campaign", *SeaWiFS Postlaunch Technical Report Series TM 2000-206892*, **8**, 46, NASA, Greenbelt, Maryland, 2000.
21. Hooker, S. B. & Morel, A. "Platform and environmental effects on above-water determinations of water-leaving radiances", *Journal of Atmospheric and Oceanic Technology*, **20**, 187-205, 2003.
22. Hooker, S. B., Lazin, G., Zibordi, G. & McLean, S. "An evaluation of above- and in-water methods for determining water-leaving radiances", *Journal of Atmospheric and Oceanic Technology*, **19**, 486-515, 2002.
23. Mobley, C. D. "Estimation of the remote-sensing reflectance from above-surface measurements", *Applied Optics*, **38**, 7442-7455, 1999.
24. Carder, K. L. & Steward, R. G. "A remote-sensing reflectance model of a red-tide dinoflagellate off west Florida", *Limnology and Oceanography*, **30**, 286-298, 1985.
25. Lee, Z. P., Carder, K. L., Peacock, T. G. & Steward, R. G., "Remote sensing reflectance measured with and without a vertical polarizer", *Ocean Optics XIII*, ed. Ackleson, S. G., 483-488, SPIE, 1997.
26. Toole, D. A., Siegel, D. A., Menzies, D. W., Neumann, M. J. & Smith, R. C. "Remote-sensing reflectance determinations in the coastal ocean: impact of instrumental characteristics and environmental variability", *Applied Optics*, **39**, 456-469, 2000.
27. Zibordi, G., Hooker, S. B., Berthon, J. F. & D'Alimonte, D. "Autonomous above-water radiance measurements from an offshore platform: a field assessment experiment", *Journal of Atmospheric and Oceanic Technology*, **19**, 808-819, 2002.
28. Hooker, S. B., Zibordi, G., Berthon, J.-F. & Brown, J. W. "Above-water radiometry in shallow coastal waters", *Applied Optics*, **43**, 4254-4268, 2004.
29. Morel, A. "In-water and remote measurements of ocean colour", *Boundary Layer Meteorology*, **18**, 177-201, 1980.
30. Deschamps, P.-Y., Fougnie, B., Frouin, R., Lecomte, P. & Verwaerde, C. "SIMBAD: A field radiometer for satellite ocean color validation", *Applied Optics*, **43**, 4055-4069, 2004.
31. Fougnie, B., Frouin, R., Lecomte, P. & Deschamps, P.-Y. "Reduction of skylight reflection effects in the above-water measurement of diffuse marine reflectance", *Applied Optics*, **38**, 3844-3856, 1999.
32. Gould, R. W., Arnone, R. A. & Sydor, M. "Absorption, scattering and remote-sensing reflectance relationships in coastal waters: testing a new inversion algorithm", *Journal of Coastal Research*, **17**, 328-341, 2001.

33. Pegau, W. S. & Zaneveld, J. R. V. "Temperature-dependent absorption of water in the red and near-infrared portions of the spectrum", *Limnology and Oceanography*, **38**, 188-192, 1993.
34. Hooker, S. B., McClain, C. R. & Holmes, A. "Ocean Color Imaging: CZCS to SeaWiFS", *Marine Technology Society*, **27**, 3-15, 1993.